European Journal of Pharmaceutics and Biopharmaceutics 137 (2019) 68–76

Contents lists available at ScienceDirect

European Journal of Pharmaceutics and Biopharmaceutics

journal homepage: www.elsevier.com/locate/ejpb

Research paper

Impact of uncharged and charged stabilizers on *in vitro* drug performances of clarithromycin nanocrystals

Suwicha Soisuwan[a], Veerawat Teeranachaideekul[a,b], Amaraporn Wongrakpanich[a,b], Peter Langguth[c], Varaporn Buraphacheep Junyaprasert[a,b,*]

[a] Department of Pharmacy, Faculty of Pharmacy, Mahidol University, Sri-Ayutthaya Road, Rajathavee, Bangkok, Thailand
[b] Center of Excellence in Innovative Drug Delivery and Nanomedicine, Faculty of Pharmacy, Mahidol University, Bangkok, Thailand
[c] Department of Pharmaceutical Technology and Biopharmaceutics, Johannes Gutenberg University, Mainz, Germany

ARTICLE INFO

Keywords:
Nanocrystal
Clarithromycin
Media milling
Surface charge
Dissolution
Solubility
Mucoadhesiveness
Drug permeation

ABSTRACT

The purpose of this study was to evaluate the effect of charge on the *in vitro* drug performances of clarithromycin nanocrystals. To prepare different charges of nanocrystals, media milling was employed with the use of different stabilizing systems. The uncharged nanocrystals were prepared from poloxamer 407. The negatively and positively charged nanocrystals were stabilized using a combination of poloxamer 407 with sodium lauryl sulfate (SLS) and cetyltrimethylammonium bromide (CTAB), respectively. After production, the particle size of the negatively and positively charged nanocrystals was smaller than that of the uncharged one. The similar particle size of variously charged clarithromycin nanocrystals was selected to determine the *in vitro* drug performances. Dissolution profiles of the variously charged nanocrystals were similar; however, kinetic saturation solubility profiles were different. The positively charged nanocrystals showed higher mucoadhesiveness than the uncharged and the negatively charged nanocrystals. For drug permeation through NCI-N87 and Caco-2 cell monolayers, both charged nanocrystals showed a higher drug transport than the uncharged nanocrystals. It could be concluded that incorporating charge into clarithromycin nanocrystal formulations affected the particle size reduction process as well as the nanocrystal performances. Therefore, the surface charge is one of the crucial factors for the development of nanocrystal formulations.

1. Introduction

The technique for enhancing drug solubility has been required for pharmaceutical formulations because approximately 40% of promising drugs in pipeline and 60% of synthetic substances have low solubility, leading to unsuccessful pharmaceutical development [1,2]. Nanocrystals are one of the techniques widely used to improve dissolution and solubility of poorly soluble drugs. Drug nanocrystals are solid drug particles in crystalline state with the particle size < 1,000 nm. These nanosized particles provide a drastic increase in surface area, resulting in the dissolution rate enhancement. Moreover, the drug solubility can be increased by reducing the particle size to the nanometer range. This is due to an increase in the particle curvature as explained by Kelvin equation [3–5].

When the nanocrystals are dispersed in liquid medium, they are referred to nanosuspensions. Nanosuspension formulation is considered a thermodynamically unstable system due to the elevation of surface energy, resulting from the dramatic increase in surface area. This system tends to reduce its energy by particle agglomeration, thus stabilizing agents are needed. In order to stabilize the nanosuspensions, two main mechanisms are involved, i.e. steric hindrance and electrostatic stabilizations. Stabilizing agents including polymers and non-ionic surfactants provide steric hindrance stabilization whereas charged stabilizers offer electrostatic stabilization by inducing surface charge which prevents the agglomeration by charge repulsion [1,6]. The stabilizing agents applied in nanocrystal formulations can be used alone or in combination [7].

Clarithromycin is the most frequently used as first-line therapy for *Helicobacter pylori* infection along with proton pump inhibitors (PPIs) and other antimicrobial drugs [8]. After PPIs administration, intra-stomach pH will be increased (pH > 4) [9]. In general, clarithromycin is chemically degraded in acid (pH 1–2), leading to rapid degradation in stomach. Therefore, co-administration of clarithromycin and PPIs can improve the chemical stability of clarithromycin [10]. Furthermore, clarithromycin is used for treatments of other bacterial infections such as respiratory tract, skin, soft tissue and sexually transmitted infections

* Corresponding author at: Department of Pharmacy, Faculty of Pharmacy, Mahidol University, 447 Sri-Ayutthaya, Rajathavee, Bangkok 10400, Thailand.
E-mail address: varaporn.jun@mahidol.ac.th (V.B. Junyaprasert).

https://doi.org/10.1016/j.ejpb.2019.02.004
Received 23 November 2018; Received in revised form 29 January 2019; Accepted 12 February 2019
Available online 12 February 2019
0939-6411/

[11] which require systemic absorption. In order to treat these diseases/conditions, the most commonly used route of administration is oral because of its convenience. However, clarithromycin is classified in Biopharmaceutical Classification System (BCS) class II which is practically insoluble in water with an acceptable permeability, resulting in low oral bioavailability. As a result, transforming clarithromycin into nanocrystals is a promising approach to solve this problem. Clarithromycin nanocrystals had been successfully prepared by sonoprecipitation [12], PLGA nanoprecipitation [13], media milling technique [14,15] and high pressure homogenization [16]. The benefits of clarithromycin nanocrystals on drug performances were reported in the previous studies [13,17] including higher anti-bacterial activity (*Staphylococcus aureus* and *Bacillus subtilis*) and higher drug permeation through gastric mucus and cell monolayers (NCI-N87 and Caco-2 cell lines) compared to clarithromycin powder and the mixture of drug and stabilizers. The superior performances of nanocrystals could be resulted from the enhancements of solubility, dissolution and adhesiveness.

The crucial factor that strongly affects nanocrystal performances is particle size [18]. According to our experience, the smaller nanocrystals provided higher saturation solubility, dissolution rate and cellular internalization than the larger ones, resulting in permeation enhancement of poorly soluble drugs [19]. Another important characteristic of nanocrystals is their surface charge which can be induced by incorporating charged stabilizers into the formulations. Positively charged nanocrystals of dexamethasone could interact with mucins, leading to an increase in the drug retention time at the absorption site [20]. Positively charged nanocrystals of atorvastatin provided higher *in vivo* anti-hyperlipidemia activity than the uncharged nanocrystals and the market product (Lipitor®) [21]. Moreover, some surfactants are known as permeation enhancers. For example, sodium lauryl sulfate (SLS), a common anionic surfactant used in nanocrystal formulations [22], is able to open tight junction of Caco-2 cell monolayer, leading to an increase in drug permeation [23]. Cationic surfactants are not a general ingredient for oral drug delivery due to their relatively high toxicity, although some of them have been reported to use as additives for oral dosage forms [24–31]. According to the previous studies, cetyltrimethylammonium bromide (CTAB) has been used in the concentration range of 0.1–1 %w/v for oral drug formulations [24–28]. This may be because it is poorly absorbed via gastrointestinal tract [32] and no toxicity after oral administration for one year was reported at low dose level (10 and 20 mg/kg/day) in rats [33]. To the best of our knowledge, CTAB used in drug nanocrystal formulation has been rarely reported. Moreover, the effect of stabilizers' charge on nanocrystal performances has not been fully elucidated. Therefore, this study aimed to evaluate the effect of uncharged and charged stabilizers on the physicochemical properties and the *in vitro* drug performances of clarithromycin nanocrystals for oral administration. Three different charges of nanocrystals were prepared using three different stabilizing systems. According to the charge of stabilizing agents at the nanocrystal surface, the obtained nanocrystals were termed as uncharged, negatively and positively charged for the nanocrystals stabilized by sole poloxamer 407, poloxamer 407 with SLS and poloxamer 407 with CTAB, respectively. All nanocrystal formulations were prepared by media milling technique using a bead milling machine. To eliminate the effect from the variation of particle size, the differently charged nanocrystals with comparable particle size were chosen for evaluating the nanocrystal performances. The physicochemical properties including particle size, zeta potential, morphology and crystallinity were determined. The differently charged nanocrystals were evaluated the *in vitro* drug performances including drug dissolution, kinetic saturation solubility, mucoadhesion and drug permeation through cultured NCI-N87 and Caco-2 cell monolayers.

2. Materials and methods

2.1. Materials

Clarithromycin was purchased from Suzhou Rovathin Foreign Trade Co., Ltd, Jiangsu, China. Poloxamer 407 and SLS were kindly supplied by BASF, Ludwigshafen, Germany. CTAB was obtained from Sigma-Aldrich, MO, USA. Glacial acetic acid was obtained from RCI-Labscan, Bangkok, Thailand. Potassium dihydrogen orthophosphate (KH_2PO_4) was gained from Fisher Scientific, Leicestershire, UK. Sodium acetate trihydrate was purchased from VWR BDH Prolabo, Leuven, Belgium. Methanol (HPLC grade) was purchased from Burdick & Jackson, NJ, USA. Porcine gastric mucins were obtained from Jiagen Biotechnologies Inc., Pierrefonds, Canada. Caco-2 (ATCC® HTB-37™) and NCI-N87 (ATCC® CRL-5822™) cell lines were provided from ATCC (American Type Culture Collection, VA, USA). Dulbecco Modified Eagle's medium (DMEM), Roswell Park Memorial Institute medium (RPMI-1640), fetal bovine serum (FBS), non-essential amino acids (NEAA), penicillin-streptomycin (Pen-strep, 10,000 U/mL), Trypsin-EDTA (0.25%) and Hank's balanced salt solution (HBSS) were purchased from Gibco, MA, USA.

2.2. Preparation of clarithromycin nanocrystals

To prepare clarithromycin nanocrystals, the media milling process was carried out using a laboratory bead milling machine (Minicer®, Netzsch, Selb, Germany) with a re-circulation mode. The milling chamber was loaded with 140 mL of grinding beads made of yttrium-stabilized zirconium oxide. Unmilled clarithromycin suspension (1%w/v) containing stabilizers was pre-milled using 0.5 mm grinding beads at the agitator speed of 2000 rpm for 5 min to roughly grind the unmilled drug into micronized particles. Then, the micronized particles were ground using 0.3 mm grinding beads at the agitator speed of 2000 rpm for 180 min. The nanosuspension was separated from the grinding beads by the screen (pore size 200 and 100 μm for 0.5 and 0.3 mm grinding beads, respectively) located in the machine. The stabilizing system for uncharged clarithromycin nanosuspension was 2%w/v poloxamer 407. The stabilizing system for negatively charged clarithromycin nanosuspension was 2%w/v poloxamer 407 and 0.1%w/v SLS [16]. For the positively charged nanosuspension, 0.1%w/v SLS was replaced with 0.1%w/v CTAB. The obtained nanosuspensions were lyophilized at −45 °C and 0.2 mbar for 24 h using a lyophilizer (Alpha 1–4, Martin Christ Gefriertrocknungsanlagen GmbH, Osterode, Germany) to acquire drug nanocrystals.

2.3. Particle size measurement

Dynamic light scattering technique using Zetasizer NanoZS (Malvern Instruments, Malvern, UK) was conducted to determine particle size and size distribution of the obtained nanocrystals. Clarithromycin nanocrystals were re-dispersed in deionized water prior the measurements. The measurements were conducted at the back scatter angle 173° and temperature of 25 °C. The average particle size (z-ave) and PDI were obtained by averaging from three measurements.

For the unmilled clarithromycin suspension, the particle size was determined by light diffraction technique using Mastersizer 2000 (Malvern Instruments, Malvern, UK). The unmilled clarithromycin suspension was dispersed in deionized water using wet sample dispersion unit with stirrer connected to the machine. The particle size was represented in volume diameter as $d_{0.5}$ which is a median of volume diameter. The average particle size was obtained from at least three measurements.

2.4. Zeta potential measurement

Surface charge of the nanocrystals depicted as zeta potential was

measured using Zetasizer NanoZS (Malvern Instruments, Malvern, UK). Clarithromycin nanocrystals were re-dispersed in conductivity adjusted deionized water (50 μS/cm). All measurements were performed at 25 °C. The average zeta potential was obtained from three measurements.

2.5. Nanocrystal morphology

Field emission scanning electron microscopy or FE-SEM (JSM-7610F, JEOL, Tokyo, Japan) was utilized to determine the nanocrystal morphology. Prior FE-SEM, the lyophilized nanocrystals were suspended in deionized water, spread and dried on a sample holder. Afterward, the dried samples were coated with platinum for 60 s under vacuum using a rotary-pumped sputter coater (Q150R, Quorum Technologies Ltd., Lewes, UK). The FE-SEM accelerating voltage was carried out at 5 kV.

2.6. Polymorphic form and crystallinity

To determine the polymorphic form and crystallinity of clarithromycin nanocrystals, two standard techniques including x-ray diffraction (XRD) and differential scanning calorimetry (DSC) were performed.

XRD was carried out using X-ray powder diffractometer (MiniFlex 600, Rigaku Corporation, Tokyo, Japan) with Cu-Kα radiation at 40 kV and 15 mA. The step scan was set at 10°/min. The diffraction patterns were shown as scattering intensity with different 2-theta (2θ) from 2°-70°. The crystallinity index (*%CI*) was calculated using peak height method [34].

DSC technique was conducted using DSC 8000 (Perkin Elmer, MA, USA). Clarithromycin nanocrystals were dispersed in deionized water and centrifuged to eliminate free stabilizers. After that, the nanocrystals were dried overnight before adding into the aluminum pan. The heating scans were set from 30 °C to 250 °C with the heating rate of 10 °C/min. The blank aluminum pan was used as a reference. The experiments were performed under nitrogen gas flow (20 mL/min). The crystallinity index (*%CI*) was derived by the following equation [35,36].

$$\%CI = \frac{\Delta H_f^{obs}}{\Delta H_f^{\hat{A}^\circ}} \times 100 \quad (1)$$

where ΔH_f^{obs} is an enthalpy of fusion of the nanocrystals and $\Delta H_f^{\hat{A}^\circ}$ is an enthalpy of fusion of the unmilled clarithromycin ($\Delta H_f^{\hat{A}^\circ} = 66.32\ J/g$).

2.7. High performance liquid chromatography (HPLC)

Clarithromycin content was quantitatively determined using HPLC instrument with UV detector (Series 20AD, Shimadzu Corporation, Kyoto, Japan). The injection volume was 50 μL. Hypersil® BDS C18 (250 mm × 4.6 mm, 5 μm) analytic column was utilized and the oven temperature was set to 40 °C. The mobile phase consisted of methanol and 50 mM phosphate buffer pH 4.0 (65:35) and the flow rate was set at 1.0 mL/min. The drug concentration was measured using UV detector at 210 nm. The HPLC condition was validated for linearity, precision and accuracy. The calibration curve was linear with the linear correlation coefficient (r^2) ≥ 0.999 at the concentration ranging from 0.5 to 100 μg/mL. The intra-day and inter-day precisions were represented as %RSD and the values were lower than 2.0%. The accuracy was represented as %recovery which fell in the range of 98–102%.

2.8. Dissolution study

USP apparatus II (paddle) dissolution tester (Erweka DT 6R, Erweka GmbH, Heusenstamm, Germany) was used for the dissolution test. In this study, the dissolution media were 900 mL of 0.10 M acetate buffer (pH 5.0) or 0.05 M phosphate buffer (pH 6.8) solution. Drug nanocrystals were weighed to have 180 mg of clarithromycin. The experiments were carried out at 37.0 ± 0.5 °C with the stirring speed of 50 rpm. The dissolution medium was withdrawn at the specific time points (2, 5, 10, 20, 30, 45, 60 and 120 min) and immediately substituted with the fresh medium at an equal volume. The collected medium was passed through filter with 0.02 μm pore size (Whatman® Anotop 25 syringe filters, Sigma-Aldrich, MO, USA). The quantitative analysis was conducted using HPLC spectroscopy as aforementioned. The experiments were performed in triplicate.

2.9. Kinetic saturation solubility

To evaluate the kinetic saturation solubility, an excess amount of clarithromycin nanocrystals were dispersed in HBSS pH 5.0 or pH 6.8. The nanosuspensions were shaken using a mechanical water bath shaker (WNB-7, Memmert GmbH, Schwbach, Germany) at 100 rpm and the temperature was set at 37.0 ± 0.5 °C. The nanosuspension was withdrawn at the specific sampling times (5 min, 1, 2, 4, 6, 12, 24, 48 and 72 h) and added into a centrifugal concentrator with MWCO 30 kDa (Vivaspin® 500, Sartorius Stedim Biotech GmbH, Goettingen, Germany). Then, the saturated solution and undissolved drug were separated by a centrifuge (Universal 320, Andreas Hettich GmbH & Co.KG (Hettich), Tuttligen, Germany) at 10,000 rpm for 8 min. The clarithromycin concentration in the ultrafiltrate was quantified using HPLC spectroscopy. The experiments were performed in triplicate.

2.10. In vitro mucoadhesion

Particle size and zeta potential of the nanocrystals were observed before and after incubation with mucins using Zetasizer NanoZS (Malvern Instruments, Malvern, UK). Clarithromycin nanocrystals were suspended in deionized water. Then, 0.5 mL of 10 mg/mL of clarithromycin nanosuspension was added into 2 mL of varied concentrations of mucins (0.03125–1.0 mg/mL). The mixtures were incubated at 37.0 ± 0.5 °C using a mechanical water bath shaker (WNB-7, Memmert GmbH, Schwbach, Germany) at 100 rpm for 2 h. The experiments were performed in triplicate.

2.11. Drug permeation

2.11.1. Cell cultures

For the permeation study, NCI-N87 and Caco-2 cell lines were chosen as representatives of gastric and intestinal cells, respectively. RPMI-1640 medium supplemented with 10% FBS and 1% Pen-strep was used as a culture medium for NCI-N87 cells. Caco-2 cells were grown in DMEM medium added with 10% FBS, 1% NEAA and 1% Pen-strep. All cell lines were incubated at 37 °C and 5% CO_2.

2.11.2. Drug permeation

NCI-N87 and Caco-2 cell lines were grown to form cell monolayer on polycarbonate membrane Transwell® inserts with the 0.4 μm pore size and 1.12 cm^2 diameter placed on a 12-well plate (Corning Life Sciences, Corning, NY, USA). The procedures were followed by the previous reports with some modifications [37,38]. The cell suspensions containing 2.5x10^5 cells of NCI-N87 cells or 1 × 10^5 cells of Caco-2 cells in the cultured media (600 μL) were seeded onto the apical side and the culture media (1,500 μL) were added in basolateral side of the Transwell®. The culture media on both sides were changed every 48 h for 20–22 days. The well plates were kept in the incubator at 37 °C and 5% CO_2. To observe the monolayer integrity, transepithelial electrical resistance (TEER, Ω.cm^2) was measured using Millicell®-ERS device with chopstick style electrodes (Millipore, MA, USA). The measuring resistance (Ω) was corrected by subtracting with the blank resistance (Ω) of the insert containing the HBSS and then multiplied by the surface area of the cell monolayer (cm^2). Cell monolayer integrity was measured before and after the experiments. TEER of the NCI-N87 and Caco-

2 monolayers used in this study were more than 70 and 350 Ω.cm^2, respectively [39,40]. Before the experiments, both apical and basolateral sides were rinsed twice with pre-warmed HBSS. Clarithromycin nanocrystals were suspended with HBSS pH 5.0 for NCI-N87 cells and HBSS pH 6.8 for Caco-2 cells. Then, 600 μL of the suspension was filled into the apical side of each Transwell®. Then, 100 μL of the nanosuspension at the apical side was taken out immediately for the initial clarithromycin concentration (C_o) determination. The 1,500 μL of fresh HBSS pH 7.4 was filled into basolateral side of the Transwell®. In order to measure the clarithromycin which was passed through the cell monolayers from the apical side to the basolateral side, 200 μL of the HBSS in the basolateral side was collected at the specific times (0, 15, 30, 60, 90 and 120 min). The fresh HBSS pH 7.4 was immediately substituted. The Transwell® well plate was kept at 37 °C on a shaker throughout the experiments. The collected samples were further quantitatively analyzed using HPLC spectroscopy. The results were represented as the cumulative amount of drug transport and the apparent permeability coefficient, P_{app} (cm/s) calculated by using the following equation.

$$P_{app} = \frac{dQ/dt}{AC_o} \quad (2)$$

where dQ/dt is a rate of clarithromycin from the apical to the basolateral sides (μg/s), A is a surface area of the cell monolayer (cm^2) and C_o is an initial concentration in the apical side (μg/mL).

2.12. Statistical analysis

The reported data were expressed as mean ± standard deviation (SD). Statistical analysis of the difference was determined using general linear model (repeated measures) followed by Bonferroni or an analysis of variance (One-Way ANOVA) followed by Tukey or Dunnett's T3 tests. All statistical tests were performed using SPSS version 21.0.0.0 (IBM Corporation, NY, USA). A p-value < 0.05 was considered significant difference.

3. Results and discussion

3.1. Preparation of various surface charges of clarithromycin nanocrystals

Three different charges of clarithromycin nanosuspensions (uncharged, negative and positive) were successfully prepared by media milling technique. For uncharged nanosuspension, poloxamer 407 was solely used as a stabilizing agent. For charged clarithromycin nanosuspension, poloxamer 407 was used in combination with SLS and CTAB to provide the negatively and positively charged clarithromycin nanosuspensions, respectively. By this method, unmilled clarithromycin was dispersed in liquid medium containing stabilizers. For bead milling process, the comminution was conducted using a re-circulation mode. Concerning the large particle size of unmilled clarithromycin, $d_{0.5}$ was 117.91 ± 12.99 μm; therefore, the pre-mill step was carried out to reduce the particle size of the unmilled drug into a few microns. After that, the obtained suspensions were ground using 0.3 mm grinding beads for 180 min.

As shown in Fig. 1, the particle size of the uncharged clarithromycin nanosuspension formulation (z-ave poloxamer 407) was initially reduced but increased drastically after 30 min of milling time (from 415.9 nm at 30 min to 1,014 nm at 180 min). In contrast, the particle sizes of the negatively and positively charged clarithromycin nanosuspension formulations were reduced during the first 90 min of milling time and remained unchanged afterward (in the ranges of 267.1–288.4 nm or 284.9–357.0 nm for the formulations containing SLS or CTAB, respectively). This indicated that addition of the steric hindrance along with electrostatic stabilization could lead to improved stability of clarithromycin nanosuspensions. These results agreed with a previous study which showed that clarithromycin nanocrystals prepared by wet milling technique could be stabilized with the use of a combination of poloxamer 407 and SLS [15]. Poloxamer 407 used as a stabilizing agent in this study, is a synthetic copolymer containing ethylene oxide and propylene oxide blocks ordered in a tri-block structure which is widely used as a non-ionic polymeric stabilizer in nanocrystal formulations. It provides steric hindrance which prevents the nanosuspensions from the aggregation and crystal growth. However, it might not be efficient to stabilize all drug nanosuspensions because the hydrophobic/hydrophilic forces are not strong enough to provide adhesion to the nanocrystal surface. For zeta potential (Table 1), the uncharged nanocrystals exhibited weak negative charge (−10 mV) due to slight ionization of hydroxyl groups of poloxamer 407. Due to the ionic surfactants in the formulation, the charged nanocrystals offered higher zeta potential compared to the uncharged nanocrystals providing more repulsive effect and prevent the particle aggregation. The previous studies reported that combining polymeric stabilizer with an ionic stabilizer resulted in a better stabilization compared to sole polymeric stabilizer [7,41–43]. Comparing between the anionic and cationic surfactants, the nanosuspension stabilized by SLS provided smaller particle size with less PDI than that stabilized by CTAB ($p < 0.05$ at 180 min milling time) (Fig. 1). Concerning the molecular weight of SLS (288.37 g/mol) and CTAB (364.45 g/mol), the molecular weight of SLS is lower than that of CTAB, providing the faster diffusion, leading to higher efficiency for covering the new nanocrystal surfaces during the production. These results were consistent with the previous studies showing that the lower molecular weight stabilizers, i.e. lower molecular weight chitosan [41], D-α-tocopherol polyethylene glycol 1000 succinate (TPGS) and SLS [44] provided higher stabilization performance. Moreover, the larger molecular size of CTAB might provide steric effect to the poloxamer chain, leading to loose packing of the stabilizer around the particle surface. This resulted in lower stabilization of the formulation containing CTAB.

To evaluate the performances of clarithromycin nanocrystals, the comparable particle size of clarithromycin nanosuspensions stabilized by the different surfactant systems were chosen. The particle size range was selected based on the obtained results from the uncharged formulation. The particle size of the uncharged formulation was smallest at 30 min of milling (415.9 ± 7.8 nm), thus this particle size range was selected. Regarding the particle sizes of negatively and positively charged clarithromycin nanosuspensions, the particle sizes of 394.4 ± 20.9 and 417.6 ± 9.9 nm, respectively, were obtained after milling for 15 min. These particle sizes were comparable to the particle size of the uncharged nanosuspension at 30 min of milling time. Therefore, the charged nanosuspensions at this time point were selected for further studies.

After production, the clarithromycin nanosuspensions were lyophilized to maintain product stability. It was found that the particle size and zeta potential of the nanosuspensions (before lyophilization) and the nanocrystals (after lyophilization) were comparable (Table 1). PDI of the differently charged nanocrystals was similar after production (before lyophilization). Normally, PDI > 0.5 indicates broad particle size distribution [45–47]. After lyophilization, PDI of the differently charged nanocrystals was acceptable (Table 1). These lyophilized nanocrystals with different charges including uncharged (C0), negative (C-) and positive (C+) charges at the selected milling times were used for the comparison studies.

FE-SEM images of the differently charged nanocrystals are shown in Fig. 2. It was found that all formulations showed a comparable particle size which was consistent with the particle size determined by Zetasizer measurement. The particle shape of the differently charged nanocrystals was cubic anisotropy.

3.2. Crystallinity of clarithromycin nanocrystals

Many polymorphic and pseudopolymorphic solvate forms of clarithromycin such as form 0 (ethanol solvate), I, II, III (acetonitrile

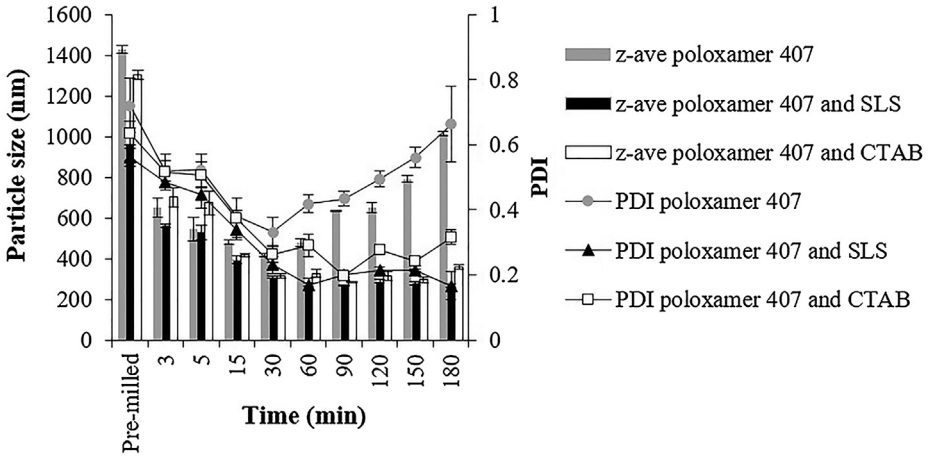

Fig. 1. Particle size (z-ave) and PDI of clarithromycin nanosuspensions stabilized by different stabilizing systems. Data are expressed as mean ± SD (n = 3).

Table 1
Particle size, PDI and zeta potential of clarithromycin nanocrystals obtained before and after lyophilization. Data are expressed as mean ± SD (n = 3).

Formulation	Particle size (nm) PDI		Zeta potential (mV)	
	Before	After	Before	After
C0	415.9 ± 7.8 0.337 ± 0.007	416.6 ± 9.0 0.244 ± 0.007	−11.5 ± 1.0	−8.3 ± 0.7
C-	394.4 ± 20.9 0.338 ± 0.023	418.6 ± 21.4 0.311 ± 0.044	−23.7 ± 1.6	−25.4 ± 0.5
C+	417.6 ± 9.9 0.372 ± 0.064	411.3 ± 15.0 0.371 ± 0.015	+19.3 ± 0.5	+24.0 ± 1.0

solvate), IV (hydrate), V, the hydrochloride salt, and the methanol solvate have been reported. Among all forms, clarithromycin form II is generally used in pharmaceutical products due to its good stability [48]. The XRD patterns of unmilled clarithromycin, each stabilizing agent, the mixtures of the drug with stabilizing agents and the various surface charges of clarithromycin nanocrystals (C0, C- and C+) are shown in Fig. 3a. The XRD pattern of unmilled clarithromycin was similar to that of clarithromycin form II which showed a distinct peak at $2\theta = 8.6^{\circ}$ [49], indicating that clarithromycin used in this study was form II. The XRD patterns of the differently charged clarithromycin nanocrystals were similar to that of its physical mixture and the unmilled clarithromycin, referring that polymorphic form was not changed by the milling process. In addition, crystallinity index obtained by XRD was semi-quantitatively analyzed by the peak height method according to Park et al. [34]. This method is simplest and most frequently used to obtain crystallinity index [50]. The results found that crystallinity of clarithromycin nanocrystals stabilized by different surfactant systems was in the same magnitude (*%CI* between 79 and 81) as shown in Table 2.

According to the DSC thermograms of unmilled clarithromycin, endothermic melting peak at 227.79 °C was found with no exothermic peak (Fig. 3b). It indicated that clarithromycin used in this study was form II [51]. The DSC thermograms of C0, C- and C+ formulations were similar to that of the unmilled drug, meaning that milling process did not change the polymorphism of clarithromycin (Fig. 3b). The obtained data from the DSC were in agreement with those from XRD. In addition, as seen in Fig. 3b, the small endothermic peak at approx. 55 °C referred to the peak of poloxamer 407 which adhered at the particle surface. In the previous studies, the decrease in ΔH_f of nanocrystals compared to that of unmilled drugs was observed [52–54]. This might be due to size reduction [55]. Therefore, to determine the crystallinity of the nanocrystals, the enthalpy of fusions of unmilled drug and the nanocrystals were compared according to Eq.1. The results revealed that *%CI* of clarithromycin nanocrystals stabilized with different surfactant systems was not different (between 90 and 97) (Table 2). Furthermore, melting peak (MP) and heat of fusion (ΔH_f) of all nanocrystals were comparable as shown in Table 2. These results indicated that the crystallinity of clarithromycin nanocrystals in this study did not depend on the surfactant systems.

3.3. Dissolution

According to the dissolution results, dissolution profiles of the differently charged nanocrystals were comparable in both pH 5.0 (gastric condition) and 6.8 (small intestine condition) dissolution media as illustrated in Fig. 4. These results indicated that surface charge did not influence the dissolution of the nanocrystals. According to the Noyes-Whitney's equation, the dissolution rate depends on the surface area of drug particles [56]. The comparable particle size of the differently

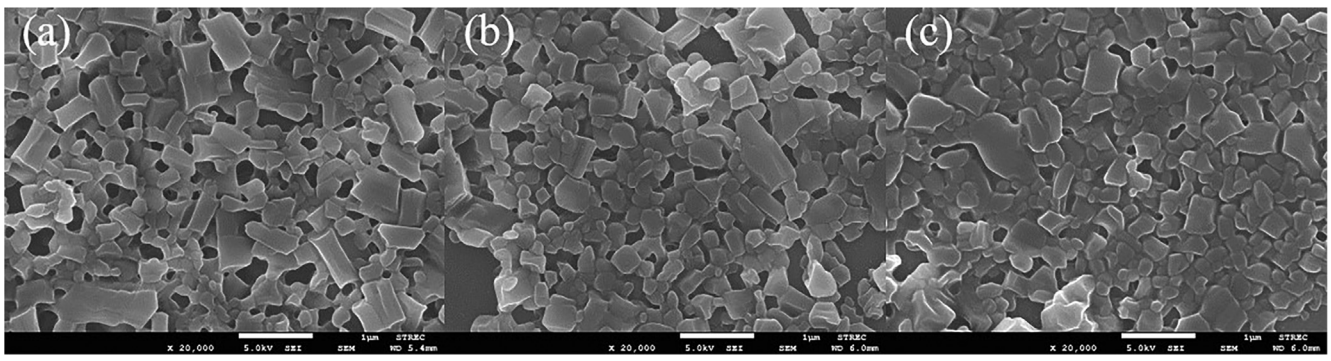

Fig. 2. FE-SEM images of C0 (a), C- (b) and C+ (c) with 20,000x magnification and 1 μm scale bar.

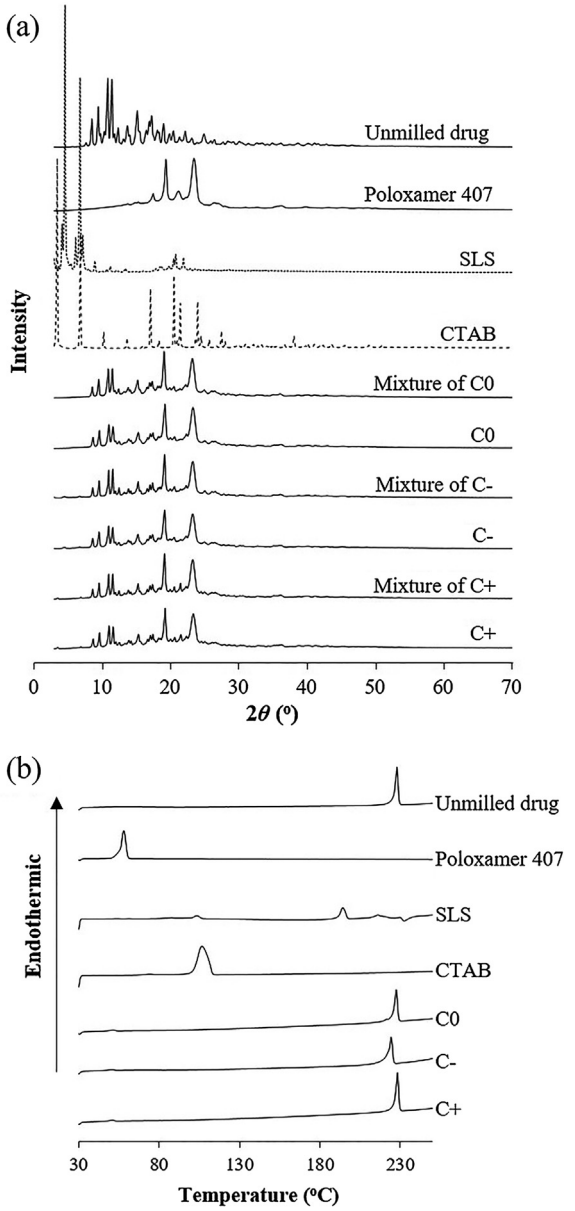

Fig. 3. XRD patterns of unmilled clarithromycin, each stabilizing agent, the mixtures of unmilled clarithromycin with stabilizing agents and the various surface charges of clarithromycin nanocrystals (a) and DSC thermograms of unmilled clarithromycin, stabilizing agents and the various surface charges of clarithromycin nanocrystals (b).

Table 2
%CI, MP and ΔH_f of the differently charged clarithormycin nanocrystals.

Formulation	*%CI*[*]	*%CI*[#]	MP (°C)[#]	ΔH_f (J/g)[#]
C0	79.89	90.90	227.33	60.2889
C-	81.11	96.04	221.72	63.6945
C+	81.76	96.19	228.08	63.7985

[*] Data were derived by the peak height method (XRD).
[#] Data were derived from DSC.

charged clarithromycin nanocrystals provided the similar surface area. Therefore, the dissolution of differently charged clarithromycin nanocrystals was similar in both pHs. Based on the obtained results, the surface charges of clarithromycin nanocrystals in this study did not affect the dissolution profile.

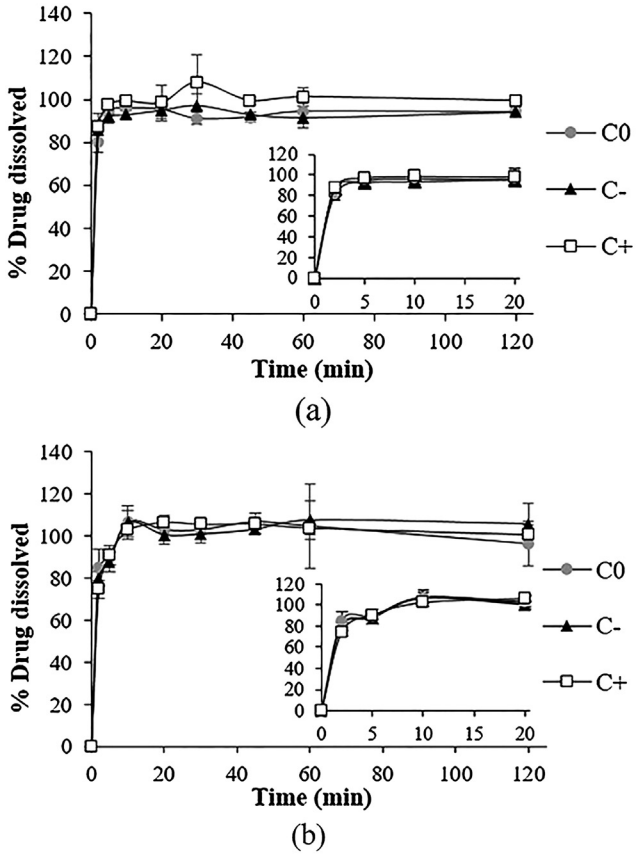

Fig. 4. Dissolution profiles of the different surface charges of clarithromycin nanocrystals in acetate buffer pH 5.0 (a) and phosphate buffer pH 6.8 (b). Data are expressed as mean ± SD (n = 3).

3.4. Kinetic saturation solubility

Although the differently charged nanocrystals had similar particle size; the kinetic saturation solubility profiles were different, as shown in Fig. 5. In both pHs, C0 exhibited the highest saturation solubility (3.73 mg/mL for pH 5.0 and 0.61 mg/mL for pH 6.8) as compared to C- (2.97 mg/mL for pH 5.0 and 0.52 mg/mL for pH 6.8) and C+ (3.70 mg/mL for pH 5.0 and 0.58 mg/mL for pH 6.8). Comparing between the charged nanocrystals, the saturation solubility of C+ was higher than that of C- in both pHs. The higher solubility of CTAB might be explained due to the lower critical micelle concentration of CTAB (0.86 mM) than SLS (4.17 mM) [57], resulting in higher micelle solubilization [15]. As a result, the saturation solubility of clarithromycin nanocrystals was influenced by the surfactant system used to stabilize the nanocrystals.

3.5. In vitro mucoadhesion

In this study, mucoadhesive properties of the differently charged clarithromycin nanocrystals were evaluated from an interaction between mucins and the nanocrystals. This interaction can lead to the change in physical characteristics including particle size and zeta potential. The particle size and zeta potential of clarithromycin nanocrystals were observed before and after exposure to different concentrations of mucins. After incubation with mucins, the particle size of C0 and C- did not change (375.2–429.0 nm) whereas that of C+ increased from 406.1 nm (no mucins) to 558.2 nm (after exposure to 1 mg/mL mucins), as shown in Fig. 6a. The significant differences in particle size of C+ relative to those of C0 and C- were observed when the nanocrystals were incubated with mucins at the concentrations equal to or greater than 0.25 mg/mL ($p < 0.05$). Regarding the surface

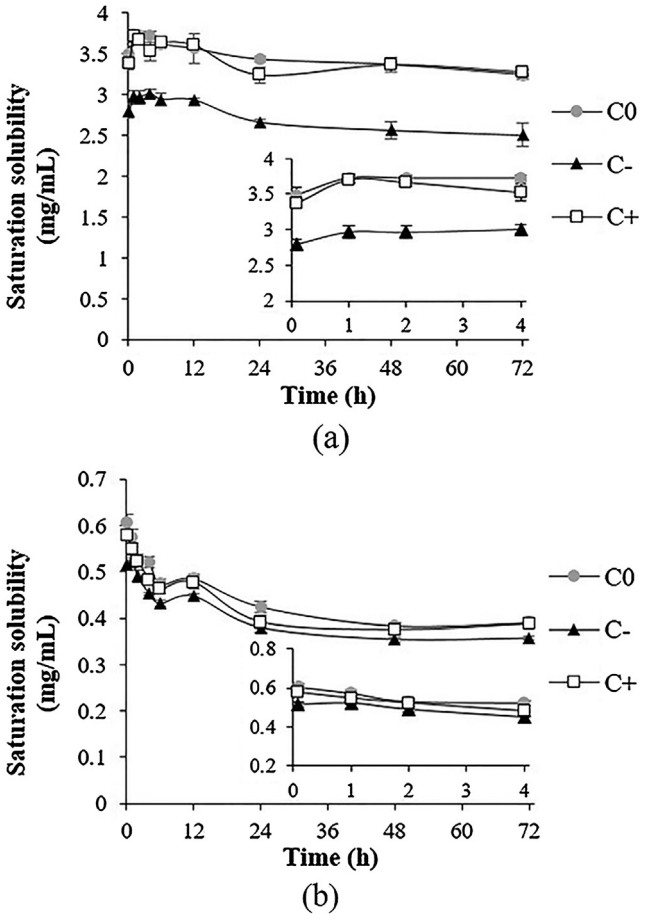

Fig. 5. Saturation solubility profiles of the different surface charges of clarithromycin nanocrystals in HBSS pH 5.0 (a) and HBSS pH 6.8 (b). Data are expressed as mean ± SD (n = 3).

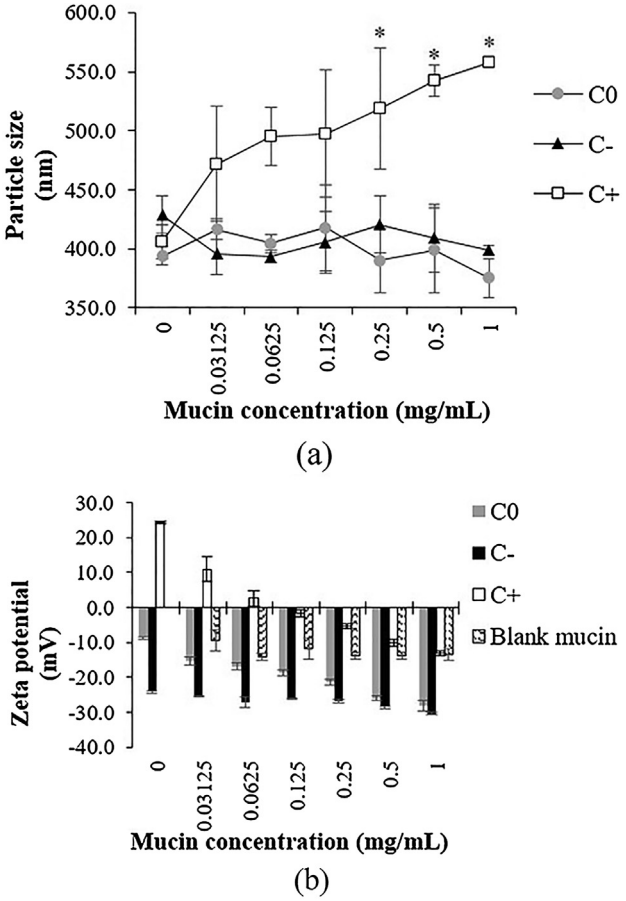

Fig. 6. Particle size (a) and zeta potential (b) of the different surface charges of clarithromycin nanocrystals after incubation with varying concentrations of mucins. Data are expressed as mean ± SD (n = 3). (*) indicates significant difference to other nanocrystal formulations ($p < 0.05$).

charge, the zeta potential of C0 and C- was slightly changed to more negative values after incubation with mucins while C+ provided dramatic change from +24.3 mV (no mucins) to −13.1 mV (1 mg/mL mucins) (Fig. 6b). The increase in particle size and the reduction in zeta potential of C+ depended on the mucin concentration. These results were consistent with the previous studies which indicated that particle size and zeta potential of the positively charged nanoparticles were altered after incubation with mucins [20,58].

The changes in the particle size and zeta potential of C+ suggested adsorption of mucins on the surface of clarithromycin nanocrystals. In general, clarithromycin has been intensively used in the treatment of *H. pylori* infection. These bacteria is able to mobilize through gastric mucus and colonize between the mucous layer and the epithelial cells [8]. Moreover, the mucous layer has also found at the tip of microvilli to cover the intestinal epithelial cells [59]. One important component of mucous layer is mucin glycoproteins which involve with viscous gel forming to cover the epithelial surface [60,61]. Mucins have negative charge in nature due to sialic acid and sulfate groups existed in their macrostructure. Therefore, positively charged particles can bind with mucins by electrostatic interaction which can prolong residence time at the active and absorption sites [59].

3.6. Drug permeation

In this study, NCI-N87 (gastric carcinoma) and Caco-2 (colorectal adenocarcinoma) cell lines were used as gastric and intestinal epithelial models, respectively, for predicting drug permeation. NCI-N87 cell line exhibits distinct stomach-like abilities such as producing gastric mucins, gastric enzymes and zymogens as well as expressing adhesion proteins such as E-cadherin and zonula occludens-1. Furthermore, NCI-N87 cells are able to form cohesive epithelium with long post-confluent stability [60]. Caco-2 cells can differentiate into monolayer with tight junctions and develop apical microvilli to resemble the intestinal epithelial cells [38,62]. To study the effect of surface charge on drug permeation, NCI-N87 and Caco-2 cell monolayers were cultured on Transwell®. The amount of drug transport and P_{app} of the C0, C− and C+ formulations were compared.

Prior to performing the drug permeation, TEER of NCI-N87 and Caco-2 cells was monitored to observe the cell monolayer integrity before and after the experiments. Clarithromycin nanocrystals at the concentration of 400 μg/mL were tested on the cell monolayers. In both cell lines, TEER value after exposure to C0 was maintained, indicating that clarithromycin and poloxamer 407 did not affect the cell monolayer integrity. For C-, TEER slightly reduced; however, it was recovered after overnight incubation with complete cultured media. This result agreed with the reversible effect of the open tight junction of SLS [23]. For NCI-N87 cell monolayer, TEER slightly decreased after being treated with C+ (400 μg/mL). In contrast, TEER of Caco-2 cell monolayer dramatically decreased after being treated with 400 μg/mL of C+ which might be due to the toxicity of CTAB. This could be explained by the ability of NCI-N87 cell line to produce gastric mucins which acted as a barrier to protect the cell monolayer [37]. Hence, the concentration of clarithromycin nanocrystals used in the drug permeation study through NCI-N87 cells was 400 μg/mL. For Caco-2 cells, the clarithromycin concentration was reduced to 200 μg/mL.

In both cell lines (Fig. 7a and b), the charged nanocrystals (C- and

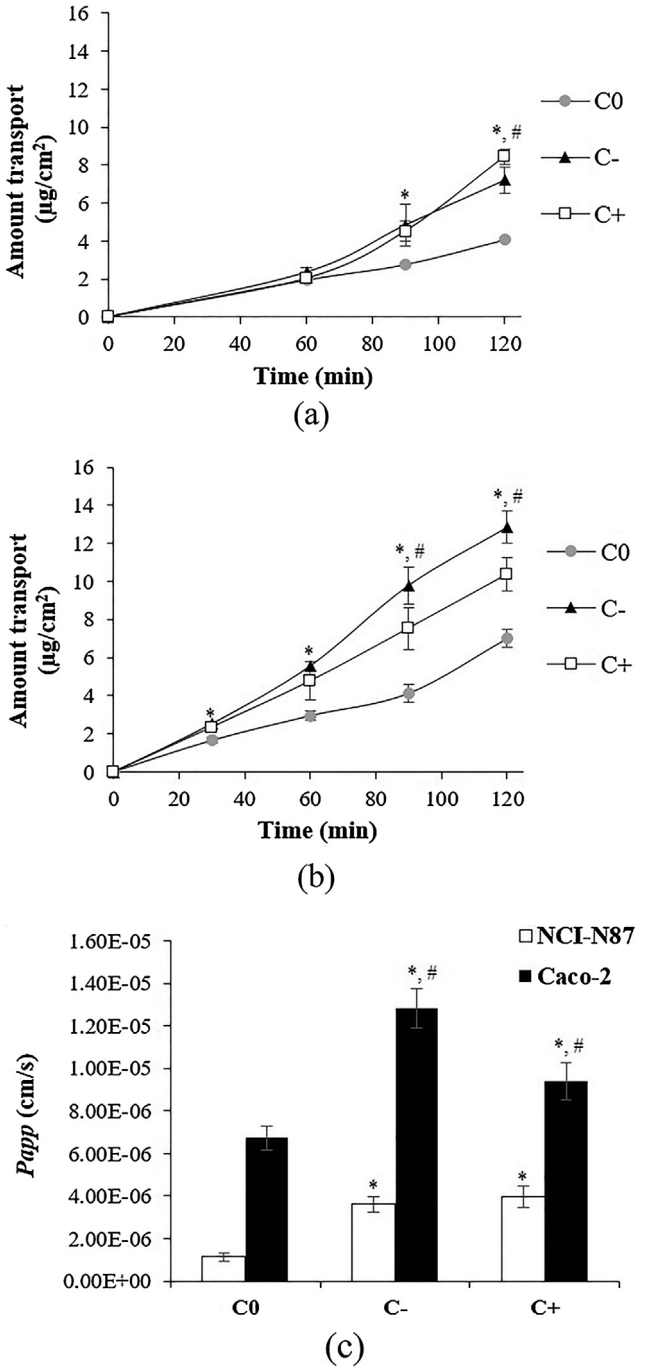

Fig. 7. Cumulative amount of drug transport of 400 μg/mL of the different charges of clarithromycin nanocrystals through NCI-N87 cell monolayer (a), 200 μg/mL of the different charges of clarithromycin nanocrystals through Caco-2 cell monolayer (b) and apparent permeability coefficient (P_{app}) (c). Data are expressed as mean ± SD (n = 4). (*) There is a significant difference between the charged and the uncharged nanocrystals. (#) There is a significant difference between the charged nanocrystals ($p < 0.05$).

C+) had the cumulative amount of drug transport significantly higher than the uncharged nanocrystals (C0). Furthermore, the P_{app} of C− and C+ was significantly higher than that of C0 as shown in Fig. 7c ($p < 0.05$). This indicated that both SLS and CTAB used in the charged nanocrystal formulations could enhance clarithromycin permeation.

Comparing between the charged nanocrystals, the amount of drug transport through NCI-N87 cell monolayer of C+ was higher than that of C- (Fig. 7a). This might be because the positive charge of C+ was able to interact with mucins produced by NCI-N87 cells. On the other hand, C- showed the significantly higher amount of drug transport (Fig. 7b) and higher P_{app} (Fig. 7c) than C+ in Caco-2 cell monolayer ($p < 0.05$). This might be due to the fact that SLS could act as a permeation enhancer by reversibly open tight junction of the Caco-2 cell monolayer [23].

4. Conclusion

Different surface charges of clarithromycin nanocrystals were successfully fabricated by media milling technique. The uncharged clarithromycin was prepared using poloxamer 407 as a non-ionic stabilizer while negative and positive charges of clarithromycin nanocrystals were stabilized by a combination of poloxamer 407 with SLS and poloxamer 407 with CTAB, respectively. Combination of stabilizing agents, i.e. poloxamer 407 with the ionic surfactant improved the milling performance. For *in vitro* drug performances, the surface charge did not affect the drug dissolution rate. However, the drug saturation solubility was influenced by different stabilizing systems. The charged nanocrystals exhibited better drug performances compared to the uncharged one. The negatively charged nanocrystals containing SLS were able to enhance drug permeation through NCI-N87 and Caco-2 cell monolayers. The positively charged nanocrystals could promote mucoadhesiveness as well as drug permeation through the cell monolayers. Therefore, it can be concluded that the surface charge is the important factor that should be concerned in the nanocrystal production because it can affect the nanocrystal performances.

Acknowledgements

This research was supported by the grant from Thai-Germance S&T Cooperation: the 2nd Call of Researcher Mobility Scheme (THAIGEM-033:ANOFID) and Mahidol University, Thailand, and the authors thank Ms. Sendra Todo for cell culture training. The authors are grateful to Asst. Prof. Dr. Toemsak Srikhirin (Department of Physics, Faculty of Sciences, Mahidol University, Bangkok, Thailand) and Netzsch (Thailand) Co., Ltd. for providing bead mill facilities.

References

[1] R. Al-Kassas, M. Bansal, J. Shaw, Nanosizing techniques for improving bioavailability of drugs, J. Control Release 260 (2017) 202–212.
[2] L. Gao, G. Liu, J. Ma, X. Wang, L. Zhou, X. Li, Drug nanocrystals: *in vivo* performances, J. Control Release 160 (2012) 418–430.
[3] D.H. Alshora, M.A. Ibrahim, F.K. Alanazi, Chapter 6 - Nanotechnology from particle size reduction to enhancing aqueous solubility, Surface Chemistry of Nanobiomaterials, William Andrew Publishing, 2016, pp. 163–191.
[4] J. Sun, F. Wang, Y. Sui, Z. She, W. Zhai, C. Wang, Y. Deng, Effect of particle size on solubility, dissolution rate, and oral bioavailability: evaluation using coenzyme Q10 as naked nanocrystals, Int. J. Nanomedicine 7 (2012) 5733–5744.
[5] J.U. Junghanns, R.H. Muller, Nanocrystal technology, drug delivery and clinical applications, Int. J. Nanomedicine 3 (2008) 295–309.
[6] B. Van Eerdenbrugh, G. Van den Mooter, P. Augustijns, Top-down production of drug nanocrystals: nanosuspension stabilization, miniaturization and transformation into solid products, Int. J. Pharm. 364 (2008) 64–75.
[7] A. Tuomela, J. Hirvonen, L. Peltonen, Stabilizing agents for drug nanocrystals: effect on bioavailability, Pharmaceutics 8 (2016) 16.
[8] D. Lopes, C. Nunes, M.C. Martins, B. Sarmento, S. Reis, Eradication of *Helicobacter pylori*: past, present and future, J. Control Release 189 (2014) 169–186.
[9] R.H. Hunt, D. Armstrong, C. James, S.K. Chowdhury, Y. Yuan, P. Fiorentini, A. Taccoen, P. Cohen, Effect on intragastric pH of a PPI with a prolonged plasma half-life: comparison between tenatoprazole and esomeprazole on the duration of acid suppression in healthy male volunteers, Am. J. Gastroenterol. 100 (2005) 1949–1956.
[10] P.O. Erah, A.F. Goddard, D.A. Barrett, P.N. Shaw, R.C. Spiller, The stability of amoxycillin, clarithromycin and metronidazole in gastric juice: relevance to the treatment of *Helicobacter pylori* infection, J. Antimicrob. Chemother. 39 (1997) 5–12.
[11] D.J. Hardy, D.R.P. Guay, R.N. Jones, Clarithromycin, a unique macrolide: a pharmacokinetic, microbiological, and clinical overview, Diagn. Microbiol. Infect. Dis. 15 (1992) 39–53.
[12] E. Esfandi, V. Ramezani, A. Vatanara, A.R. Najafabadi, S.P.H. Moghaddam, Clarithromycin dissolution enhancement by preparation of aqueous

nanosuspensions using sonoprecipitation technique, Iran. J. Pharm. Res. 13 (2014) 809–818.
[13] G. Mohammadi, A. Nokhodchi, M. Barzegar-Jalali, F. Lotfipour, K. Adibkia, N. Ehyaei, H. Valizadeh, Physicochemical and anti-bacterial performance characterization of clarithromycin nanoparticles as colloidal drug delivery system, Coll. Surf. B Biointerf. 88 (2011) 39–44.
[14] M. Shahbaziniaz, S.M. Foroutan, N. Bolourchian, Dissolution rate enhancement of clarithromycin using ternary ground mixtures: nanocrystal formation, Iran. J. Pharm. Res. 12 (2013) 587–598.
[15] M.S. Niaz, D. Traini, P.M. Young, M. Ghadiri, R. Rohanizadeh, Investigation into physical-chemical variables affecting the manufacture and dissolution of wet-milled clarithromycin nanoparticles, Pharm. Dev. Technol. 19 (2014) 911–921.
[16] B. Morakul, J. Suksiriworapong, J. Leanpolchareanchai, V.B. Junyaprasert, Precipitation-Lyophilization-Homogenization (PLH) for preparation of clarithromycin nanocrystals: influencing factors on physicochemical properties and stability, Int. J. Pharm. 457 (2013) 187–196.
[17] B. Morakul, J. Suksiriworapong, M.T. Chomnawang, P. Langguth, V.B. Junyaprasert, Dissolution enhancement and *in vitro* performance of clarithromycin nanocrystals produced by precipitation–lyophilization–homogenization method, Eur. J. Pharm. Biopharm. 88 (2014) 886–896.
[18] G. Sandri, M.C. Bonferoni, F. Ferrari, S. Rossi, C.M. Caramella, The role of particle size in drug release and absorption, in: H.G. Merkus, G.M.H. Meesters (Eds.), Particulate products: tailoring properties for optimal performance, Springer International Publishing, Cham, 2014, pp. 323–341.
[19] S. Soisuwan, V. Teeranachaideekul, A. Wongrakpanich, P. Langguth, V.B. Junyaprasert, *In vitro* performances and cellular uptake of clarithromycin nanocrystals produced by media milling technique, Powder Technol. 338 (2018) 471–480.
[20] G.B. Romero, C.M. Keck, R.H. Muller, N.A. Bou-Chacra, Development of cationic nanocrystals for ocular delivery, Eur. J. Pharm. Biopharm. 107 (2016) 215–222.
[21] M. Kurakula, A.M. El-Helw, T.R. Sobahi, M.Y. Abdelaal, Chitosan based atorvastatin nanocrystals: effect of cationic charge on particle size, formulation stability, and *in-vivo* efficacy, Int. J. Nanomedicine 10 (2015) 321–334.
[22] E. Merisko-Liversidge, G.G. Liversidge, Nanosizing for oral and parenteral drug delivery: a perspective on formulating poorly-water soluble compounds using wet media milling technology, Adv. Drug Deliv. Rev. 63 (2011) 427–440.
[23] E.K. Anderberg, P. Artursson, Epithelial transport of drugs in cell culture. VIII: effects of sodium dodecyl sulfate on cell membrane and tight junction permeability in human intestinal epithelial (Caco-2) cells, J. Pharm. Sci. 82 (1993) 392–398.
[24] P. Khachane, A.A. Date, M.S. Nagarsenker, Positively charged polymeric nanoparticles: application in improving therapeutic efficacy of meloxicam after oral administration, Pharmazie 66 (2011) 334–338.
[25] A. Ramadan, F. Lagarce, A. Tessier-Marteau, O. Thomas, P. Legras, L. Macchi, P. Saulnier, J.P. Benoit, Oral fondaparinux: use of lipid nanocapsules as nanocarriers and *in vivo* pharmacokinetic study, Int. J. Nanomed. 6 (2011) 2941–2951.
[26] G. Arzani, A. Haeri, M. Daeihamed, H. Bakhtiari-Kaboutaraki, S. Dadashzadeh, Niosomal carriers enhance oral bioavailability of carvedilol: effects of bile salt-enriched vesicles and carrier surface charge, Int. J. Nanomed. 10 (2015) 4797–4813.
[27] M.M. Eissa, R.M. El-Moslemany, A.A. Ramadan, E.I. Amer, M.Z. El-Azzouni, L.K. El-Khordagui, Miltefosine lipid nanocapsules for single dose oral treatment of *Schistosomiasis mansoni*: a preclinical study, PLoS. ONE 10 (2015) e0141788.
[28] Z. Shao, Y. Li, R. Krishnamoorthy, T. Chermak, A.K. Mitra, Differential effects of anionic, cationic, nonionic, and physiologic surfactants on the dissociation, alpha-chymotryptic degradation, and enteral absorption of insulin hexamers, Pharm. Res. 10 (1993) 243–251.
[29] S. Hariharan, V. Bhardwaj, I. Bala, J. Sitterberg, U. Bakowsky, M.N. Ravi Kumar, Design of estradiol loaded PLGA nanoparticulate formulations: a potential oral delivery system for hormone therapy, Pharm. Res. 23 (2006) 184–195.
[30] V. Bhardwaj, D.D. Ankola, S.C. Gupta, M. Schneider, C.M. Lehr, M.N. Kumar, PLGA nanoparticles stabilized with cationic surfactant: safety studies and application in oral delivery of paclitaxel to treat chemical-induced breast cancer in rat, Pharm. Res. 26 (2009) 2495–2503.
[31] H. Chen, Y. Zheng, G. Tian, Y. Tian, X. Zeng, G. Liu, K. Liu, L. Li, Z. Li, L. Mei, L. Huang, Oral delivery of DMAB-modified docetaxel-loaded PLGA-TPGS nanoparticles for cancer chemotherapy, Nanoscale Res. Lett. 6 (2011) 4.
[32] B. Isomaa, Absorption, distribution and excretion of [^{14}C]CTAB, a quaternary ammonium surfactant, in the rat, Food Cosmet. Toxicol. 13 (1975) 231–237.
[33] B. Isomaa, J. Reuter, B.M. Djupsund, The subacute and chronic toxicity of cetyltrimethylammonium bromide (CTAB), a cationic surfactant, in the rat, Arch. Toxicol. 35 (1976) 91–96.
[34] S. Park, J.O. Baker, M.E. Himmel, P.A. Parilla, D.K. Johnson, Cellulose crystallinity index: measurement techniques and their impact on interpreting cellulase performance, Biotechnol. Biofuels 3 (2010) 10.
[35] V. Teeranachaideekul, T. Chantaburanan, V.B. Junyaprasert, Influence of state and crystallinity of lipid matrix on physicochemical properties and permeation of capsaicin-loaded lipid nanoparticles for topical delivery, J. Drug Deliv. Sci. Technol. 39 (2017) 300–307.
[36] V. Teeranachaideekul, R.H. Müller, V.B. Junyaprasert, Encapsulation of ascorbyl palmitate in nanostructured lipid carriers (NLC)—Effects of formulation parameters on physicochemical stability, Int. J. Pharm. 340 (2007) 198–206.
[37] M. Lemieux, P. Gosselin, M.A. Mateescu, Carboxymethyl starch mucoadhesive microspheres as gastroretentive dosage form, Int. J. Pharm. 496 (2015) 497–508.
[38] I. Hubatsch, E.G. Ragnarsson, P. Artursson, Determination of drug permeability and prediction of drug absorption in Caco-2 monolayers, Nat. Protoc. 2 (2007) 2111–2119.
[39] H. Qiao, L. Chen, T. Rui, J. Wang, T. Chen, T. Fu, J. Li, L. Di, Fabrication and *in vitro/in vivo* evaluation of amorphous andrographolide nanosuspensions stabilized by D-α-tocopheryl polyethylene glycol 1000 succinate/sodium lauryl sulfate, Int. J. Nanomedicine 12 (2017) 1033–1046.
[40] K. Saraiva-Pava, N. Navabi, E.C. Skoog, S.K. Linden, M. Oleastro, M. Roxo-Rosa, New NCI-N87-derived human gastric epithelial line after human telomerase catalytic subunit over-expression, World J. Gastroenterol. 21 (2015) 6526–6542.
[41] W. Sun, W. Tian, Y. Zhang, J. He, S. Mao, L. Fang, Effect of novel stabilizers—cationic polymers on the particle size and physical stability of poorly soluble drug nanocrystals, Nanomedicine 8 (2012) 460–467.
[42] F. Li, L. Li, S. Wang, Y. Yang, J. Li, D. Liu, S. Zhang, S. Wang, H. Xu, Improved dissolution and oral absorption by co-grinding active drug probucol and ternary stabilizers mixtures with planetary beads-milling method, AJPS (2018).
[43] S. Huang, Q. Zhang, H. Li, Y. Sun, G. Cheng, M. Zou, H. Piao, Increased bioavailability of efonidipine hydrochloride nanosuspensions by the wet-milling method, Eur. J. Pharm. Biopharm. 130 (2018) 108–114.
[44] H. Rachmawati, L. Al Shaal, R.H. Muller, C.M. Keck, Development of curcumin nanocrystal: physical aspects, J. Pharm. Sci. 102 (2013) 204–214.
[45] T. Zhou, Z. Lin, P. Puligujja, D. Palandri, J. Hilaire, M. Araínga, N. Smith, N. Gautam, J. McMillan, Y. Alnouti, X. Liu, B. Edagwa, H.E. Gendelman, Optimizing the preparation and stability of decorated antiretroviral drug nanocrystals, Nanomedicine 13 (2018) 871–885.
[46] R. Narayan, A. Pednekar, D. Bhuyan, C. Gowda, K.B. Koteshwara, U.Y. Nayak, A top-down technique to improve the solubility and bioavailability of aceclofenac: *in vitro* and *in vivo* studies, Int. J. Nanomed. 12 (2017) 4921–4935.
[47] X. Ye, H. Patil, X. Feng, R.V. Tiwari, J. Lu, A. Gryczke, K. Kolter, N. Langley, S. Majumdar, D. Neupane, S.R. Mishra, M.A. Repka, Conjugation of hot-melt extrusion with high-pressure homogenization: a novel method of continuously preparing nanocrystal solid dispersions, AAPS PharmSciTech 17 (2016) 78–88.
[48] S. Noguchi, K. Takiyama, S. Fujiki, Y. Iwao, K. Miura, S. Itai, Polymorphic transformation of antibiotic clarithromycin under acidic condition, J. Pharm. Sci. 103 (2014) 580–586.
[49] Y. Tozuka, A. Ito, H. Seki, T. Oguchi, K. Yamamoto, Characterization and quantitation of clarithromycin polymorphs by powder X-ray diffractometry and solid-state NMR spectroscopy, Chem. Pharm. Bull. 50 (2002) 1128–1130.
[50] X. Ju, M. Bowden, E.E. Brown, X. Zhang, An improved X-ray diffraction method for cellulose crystallinity measurement, Carbohydr. Polym. 123 (2015) 476–481.
[51] Y.T. Sohn, J.K. Rhee, W.B. Im, Polymorphism of clarithromycin, Arch. Pharm. Res. 23 (2000) 381–384.
[52] K.D. Koradia, R.H. Parikh, H.D. Koradia, Albendazole nanocrystals: Optimization, spectroscopic, thermal and anthelmintic studies, J. Drug Deliv. Sci. Technol. 43 (2018) 369–378.
[53] A. Otte, M.T. Carvajal, Assessment of milling-induced disorder of two pharmaceutical compounds, J. Pharm. Sci. 100 (2011) 1793–1804.
[54] P. Sharma, W.A. Denny, S. Garg, Effect of wet milling process on the solid state of indomethacin and simvastatin, Int. J. Pharm. 380 (2009) 40–48.
[55] Q. Yu, X. Wu, Q. Zhu, W. Wu, Z. Chen, Y. Li, Y. Lu, Enhanced transdermal delivery of meloxicam by nanocrystals: preparation, *in vitro* and *in vivo* evaluation, AJPS 13 (2018) 518–526.
[56] A.A. Noyes, W.R. Whitney, The rate of solution of solid substances in their own solutions, J. Am. Chem. Soc. 19 (1897) 930–934.
[57] T.J.V. Prazeres, M. Beija, F.V. Fernandes, P.G.A. Marcelino, J.P.S. Farinha, J.M.G. Martinho, Determination of the critical micelle concentration of surfactants and amphiphilic block copolymers using coumarin 153, Inorganica Chim. Acta 381 (2012) 181–187.
[58] I. Pereira de Sousa, C. Steiner, M. Schmutzler, M.D. Wilcox, G.J. Veldhuis, J.P. Pearson, C.W. Huck, W. Salvenmoser, A. Bernkop-Schnurch, Mucus permeating carriers: formulation and characterization of highly densely charged nanoparticles, Eur. J. Pharm. Biopharm. 97 (2015) 273–279.
[59] C. Gamazo, N. Martin-Arbella, A. Brotons, A.I. Camacho, J.M. Irache, Mimicking microbial strategies for the design of mucus-permeating nanoparticles for oral immunization, Eur. J. Pharm. Biopharm. 96 (2015) 454–463.
[60] T.d. Santos, B.N. Lourenço, J. Coentro, P.L. Granja, 3.2 - Cell-based *in vitro* models for gastric permeability studies, Concepts and models for drug permeability studies, Woodhead Publishing, 2016, pp. 41–56.
[61] V.N. Boya, R. Lovett, S. Setua, V. Gandhi, P.K.B. Nagesh, S. Khan, M. Jaggi, M.M. Yallapu, S.C. Chauhan, Probing mucin interaction behavior of magnetic nanoparticles, J. Coll. Interf. Sci. 488 (2017) 258–268.
[62] C. Pereira, J. Costa, B. Sarmento, F. Araújo, 3.3 - Cell-based *in vitro* models for intestinal permeability studies, Concepts and models for drug permeability studies, Woodhead Publishing, 2016, pp. 57–81.